Etching behavior of Si(001)-2×1 studied with optical anisotropy

D. J. Wentink
Solid State Division, Centre for Materials Research, University of Twente, P.O. Box 217, 7500 AE Enschede, The Netherlands and Hoogovens Research and Development, Bnuiden, The Netherlands

M. Kuijper, H. Wormeester, and A. van Silfhout
Solid State Division, Centre for Materials Research, University of Twente, P.O. Box 217, 7500 AE Enschede, The Netherlands
(Received 13 March 1997)

Etching of single-domain Si(001)-2×1 by 800-eV Ar^+ ions has been studied using surface-induced optical-anisotropy measurements in the temperature range from 293 to 870 K. At 293 K, the surface area which is distorted by one impinging ion is determined to be 3.9×10^{-14} cm^2, and at this temperature no annealing was observed. With increasing temperatures the etch behavior gradually changes from mere roughening to a situation where ion-induced surface damage is restored. At 670 K and 10^{11} ions $cm^{-2}s^{-1}$, no ion-induced changes in the optical anisotropy could be observed, and hence D_B step etching occurs. During ion bombardment at higher temperatures we observed the development of protrusions on the surface with facets in the $\{11l\}$ directions. Protrusions were also found during etching by O_2 at 1020 K, and their development is attributed to pinning at residual contaminations. Formation of protrusions during sample cleaning may be responsible for the large scatter in reported optical-anisotropy data of clean single-domain Si(001)-2×1. This illustrates the importance of a well-controlled sample preparation procedure. [S0163-1829(97)06336-4]

I. INTRODUCTION

Cleaning of Si(001) surfaces usually involves an etch stage during flash annealing or ion bombardment. Usually little attention is paid to the effect of such an etch stage on surface morphology. Nevertheless, this effect can be considerable: low-energy Xe-ion bombardment can force Si(001)-2×1 from its equilibrium double-domain configuration to a metastable configuration with only one domain and double height steps.[1] On the other hand, a flash anneal treatment at 1400 K may yield large pyramidal protrusions on the surface with $\{11l\}$-oriented facets.[2] These examples illustrate that, besides the importance of etch phenomena in, for example, ion-beam-stimulated growth techniques,[3] knowledge and control of these phenomena are vital for preparing well-defined Si(001) surfaces for fundamental studies of surface morphology.

Measurements of optical reflection properties of materials during growth are a well-established tool in determining and controlling composition and/or growth rate.[4] When optical reflection is measured with the incoming light beam at a normal angle of incidence, it becomes possible to probe optical anisotropy of substrate and surface. By following the change in surface-induced optical anisotropy (SIOA) due to the increase and decrease of dimer-related anisotropy on (001) surfaces of III-V materials, the amount of deposited material can be determined with submonolayer precision. This makes SIOA and reflection high-energy electron-diffraction competitive growth monitors in III-V material growth.[5] On nominally (001)-oriented group-IV materials, the number of dimers oriented along [110] and [$\bar{1}$10] is usually the same. Hence, laterally averaged, the dimer-related SIOA on these surfaces cancels. Therefore, (001) surfaces of group-IV semiconductors require special preparation to bring out dimer-related optical anisotropy. This is the reason why there are only a few SIOA studies on Si and Ge(001) surfaces. In this work the sensitivity of SIOA to surface morphology is exploited to obtain real-time *in situ* information about the influence of etching on single-domain Si(001)-2×1.

On Si and Ge(001), domains where dimer bonds are normal to and along step edges are labeled *A* and *B* domains, respectively. Steps are labeled after the domain on the upper terrace, $S_{A(B)}$ and $D_{A(B)}$ for single and double height steps respectively. On nominal (001)-oriented Si or Ge, all steps are of single height and the area covered by the two domains is equal. By manipulating the surface, the area of one of the domains can be enhanced at the expense of the other domain. This can be done by applying external stress,[6] homoepitaxial growth,[7] etching by low-energy ions,[1] or using substrates[8] oriented a few degrees toward [110]. For growth (etching), a larger growth (removal) rate of S_B steps is the underlying mechanism which can force the surface into a single-domain configuration. External applied stress, as well as slightly off-oriented (001) substrates tend to a single-domain configuration due to a trade off between step energies and accommodation of surface stress. To the best of our knowledge, all available optical anisotropy data of single-domain Si(001)-2×1 have been obtained from substrates oriented a few degrees toward [110]. Nevertheless, there is considerable scatter in the obtained SIOA spectra, both in the size and shape of these spectra.[9–12] The underlying origin of these differences might be attributed to the various sample preparation methods used.

II. EXPERIMENT

Experiments were performed on Si(001) substrates with miscut angles of $4.4\pm0.1°$ and $0.0\pm0.1°$ toward [110] and [$\bar{1}$10], respectively, and 10^{13} B m^{-3}. Background pressures

were below 10^{-8} Pa. Sample temperatures were established using two-wavelength infrared and optical pyrometry. After correcting for the emissivity, obtained sample temperatures were fitted into a model which incorporates thermal radiation and conduction and dc input power. This results in a final accuracy of[13,14] ± 15 K. Prior to mounting, samples were ultrasonically rinsed in 2-propanol, followed by 12-h *in situ* outgassing at temperatures up to 600 K, while the pressure was maintained below 10^{-7} Pa. Final cleanliness was achieved by ion bombardment (Ar^+, 800 eV, 10^{12} ions cm^{-2} s^{-1}, 20 min), followed by 1-h annealing at 1100 K. This yields contamination levels below the Auger detection limit.

SIOA measurements were performed by operating an ellipsometer at a near-normal angle of incidence using a broadband optical compensator.[14,15] By measuring the ellipsometric signal of an initial (i) and modified (m) surface, the change in SIOA is obtained according to[16]

$$[1+\delta\tan(\psi)]\exp(i\delta\Delta)\equiv\frac{r^{i}_{[\bar{1}10]}r^{m}_{[110]}}{r^{i}_{[110]}r^{m}_{[\bar{1}10]}}, \qquad (1)$$

where r is the reflection coefficient of normal incident light, with linear polarization along the indicated crystal axis. The initial surface is clean, single-domain Si(001)-2×1, and the modification is etching with either 800-eV Ar ions or O_2. Both $\delta\tan(\psi)$ and $\delta\Delta$ are measured at photon energies between 1.5 and 5.0 eV. Here we will concentrate on $\delta\tan(\psi)$, since $\delta\tan(\psi)$ and $\delta\Delta$ are related by a Kramers-Kronig transformation, and for the work here $\delta\Delta$ does not give additional information.

III. ROOM-TEMPERATURE ION BOMBARDMENT

Normal angle of incidence ellipsometric results at 293 K of single-domain Ge(001)-2×1 showed that changes in optical anisotropy measured upon 800-eV Ar-ion bombardment or O_2 exposure are identical.[17] From this it was concluded that either of these surface modifications yields an optical isotropic surface, i.e., $r^{m}_{[110]}=r^{m}_{[\bar{1}10]}$. Then, by taking the modulus of Eq. (1), we obtain

$$\delta\tan(\psi)=\frac{|r^{i}_{[\bar{1}10]}|-|r^{i}_{[110]}|}{|r^{i}_{[110]}|}. \qquad (2)$$

The conclusion that either oxidation or ion bombardment of Ge(001)-2×1 produce the same optical anisotropy is confirmed by reflectance difference spectroscopy (RDS) measurements, where the right-hand side of Eq. (2) is measured directly. SIOA and RDS data of single-domain Ge(001)-2×1 are essentially the same.[9,16–18] Scanning tunnelling microscopy and molecular dynamics studies of Si(001)-2×1 during and after low-dose Ar-ion bombardment reveal surface roughening by this treatment.[19,20] Therefore, Si(001)-2×1 is expected to be optical isotropic after 800-eV Ar-ion bombardment at 293 K. In Fig. 1 the change in optical anisotropy of single-domain Si(001)-2×1, measured upon ion bombardment, is given.

There are several studies which report the SIOA spectrum of Si(001)-2×1 at room temperature.[9–12] As in Fig. 1, they

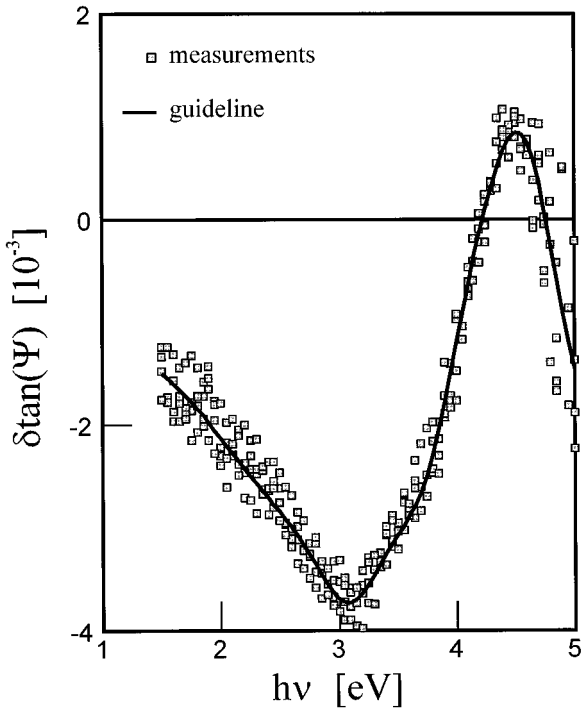

FIG. 1. Optical anisotropy of single-domain Si(001)-2×1. The modification is an 800-eV Ar-ion bombardment at 293 K with a flux of 2×10^{11} or 2×10^{12} ions $cm^{-2}s^{-1}$ for 10^3 s. For these fluences the signal size is not affected by the differences therein.

all exhibit a negative peak near 3.1 eV, a shoulder near 3.8 eV, and a positive peak near 4.5 eV. Although the overall agreement between the various spectra is reasonable there are also a number of discrepancies in the energy positions of the extrema and in peak heights. The spread in energy positions of the peaks might be due to the sensitivity of SIOA spectra to chemical contaminations, as already mentioned in Refs. 9–12. Chemisorbed species on single-domain Si(001)-2×1 are found to exhibit optical anisotropy at photon energies in excess of 3 eV, while almost no optical anisotropy is found below this photon energy. This was found for various adsorbates like H,[11,14,21] H_2O,[14] and As.[10] Since the characteristic features of SIOA spectra of Si(001)-2×1 are also above 3 eV, the shape of these spectra will be critically dependent on surface cleanliness. We studied the effect of uncontrolled surface contamination by repeating the experiment on the same specimen, as well as on different specimens. Furthermore we created an isotropic reference substrate by oxidizing it with O_2 rather than modification with Ar ions. In all cases we observed SIOA spectra identical to that of Fig. 1 within the experimental error. Combined with contamination levels below the Auger detection limit, we found no evidence of chemical contaminations on our spectrum. Another interesting point is the amount of optical anisotropy. For samples with miscut angles similar to our substrates, anisotropies of the 3.1-eV peak are reported in the range of[9–12] -1.5×10^{-3} to -2.5×10^{-3}. However, in Fig. 1 it is -3.8×10^{-3}. Apart from the possibility of a decreased anisotropy due to surface contamination, such a decrease can be caused by differences in the domain ratio due to surface preparation. This suggests that our cleaning procedure yields an almost single-domain surface, and that the amount of op-

tical anisotropy of Si(001)-2×1 is commonly underestimated. This point will be addressed in Sec. V.

The origin of SIOA signals is still a matter of debate. Optical transitions from surface-to-surface, surface-to-bulk, bulk-to-surface, and even bulk-to-bulk states need to be considered. Also, a subtle relation between surface optical transitions and propagation of electromagnetic waves may be involved.[22] Nevertheless, optical anisotropy of Si(001)-2×1 must be related to an anisotropic structure. On Si(001)-2×1, oriented 4.4° toward [110], there are two anisotropic features: dimers and steps. There are indications that optical-anisotropy spectra of dimerized surfaces are related to energy positions of surface states, though the precise relation is still being discussed.[10,16,17,23] Furthermore, it has been demonstrated that on As-passivated Si(001)-2×1 the optical anisotropy changes sign, while spectral features are retained, if the As-As dimer bond is rotated over 90°. This indicates that the SIOA signal originates from the surface reconstruction, e.g., dimers, and not from steps. By attributing the SIOA signal solely to dimers, the optical anisotropy becomes linear with the excess fraction δf of one domain with respect to the other according to

$$\frac{|r_{[1\bar{1}0]}|-|r_{[110]}|}{|r_{[110]}|}\propto\delta f\equiv f_B-f_A, \tag{3}$$

where f_A and f_B are the surface fractions covered with A and B domains, respectively. In general we have $f_A+f_B+f_R=1$, where f_R is the surface fraction without A or B domains, like steps, contaminants, roughened area, etc. For a perfect single B domain surface $f_B=1$ and $f_A=f_R=0$, and an anisotropy signal can be expected whereas a surface, completely roughened by ion bombardment, has $f_R=1$, and hence $f_A=f_B=0$, e.g., no optical anisotropy. Consequently, the SIOA signal can be used to measure the domain excess fraction δf.

The behavior of $\delta\tan(\psi)$ vs ion dose may reveal information about the sputter process and/or the SIOA origin. A possible model for the SIOA signal during ion bombardment is that one ion roughens an area A_S. If we split the surface in a fraction contributing to the SIOA signal, ξ_C, and a fraction which does not contribute, $1-\xi_C$, and assume that an area already roughened by an ion does not contribute to the SIOA signal anymore, then the time evolution of ξ_C is given by

$$\xi_C(t)=\xi_C(0)\exp(-\Phi A_S t), \tag{4}$$

where Φ is the Ar ion flux and A_s is the area roughened by one Ar ion. With the linear relation between ξ_C and the SIOA signal, e.g., $\xi_C\propto\delta f$, we obtain for the SIOA signal during ion bombardment at 293 K:

$$\frac{\delta\tan[\psi(h\nu)]_{\rm iso}-\delta\tan[\psi(h\nu,t)]}{\delta\tan[\psi(h\nu)]_{\rm iso}}\approx\frac{\xi_C(t)}{\xi_C(0)}=\exp(-\Phi A_S t); \tag{5}$$

see also Eqs. (1), (3), and (4). In Eq. (5), $\delta\tan[\psi(h\nu)]_{\rm iso}$ is the signal when all optical anisotropy is removed by ion bombardment, i.e., $\xi_C=\delta f=0$.

The SIOA signal was followed during Ar-ion bombardment at 293 K; see Fig. 2 for measurements at $h\nu=3.5\,eV$. The fit in Fig. 2 is a least-squares fit using Eq. (5), with A_S as only fit parameter and $\delta\tan[\psi(h\nu)]_{\rm iso}$ is obtained from Fig. 1 by taking $\delta\tan(\psi)$ at 3.5 eV. The ion flux in Figs. 1 and 2 differs more than an order of magnitude. Nevertheless, the values of $\delta\tan[\psi(h\nu)]_{\rm iso}$ are identical in both experiments, which shows that anneal effects at 293 K are insignificant. Hence, roughening due to impeding ions can be described by an area A_S of permanently displaced atoms. The model predicts the same behavior for $\delta\tan(\psi)$ at different photon energies. Measurements at various energies yield the same value of A_S within 5%, and from Fig. 2 we derive an area $A_S=3.9\times10^{-14}$ cm^2, which is equivalent to 26 ± 2 first-layer atoms.

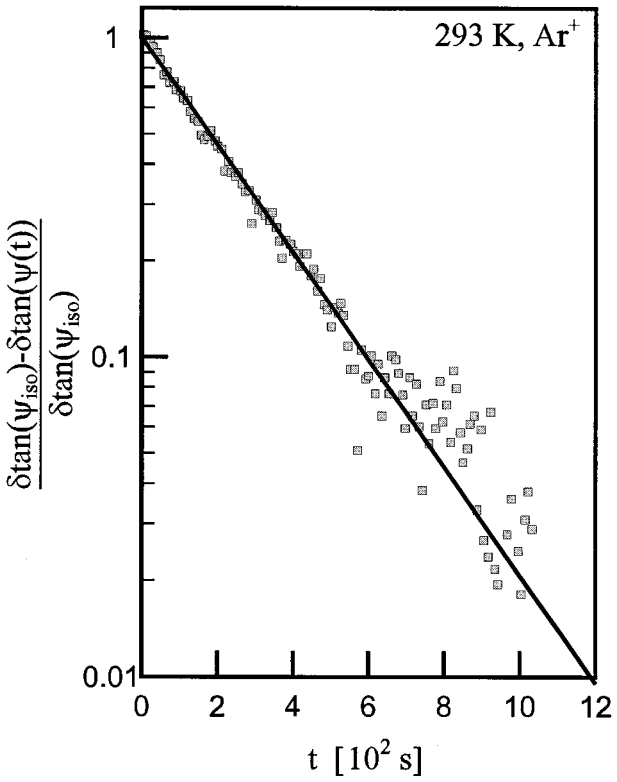

FIG. 2. Behavior of the SIOA signal at photon energy 3.5 eV upon 800-eV Ar-ion bombardment. Sample temperature 293 K, 10^{11} ions cm^{-2} s^{-1}. Squares: measurements; line: fit according to Eq. (5).

Similar experiments on Si(001)-2×1, where damage imposed by a low-dose 3-keV Ar-ion bombardment was studied with scanning tunneling microscopy and molecular-dynamics simulations, show that one ion creates, on average, six defects of different sizes.[19,20] With an average damage/defect of two dimers, this yields a damage of 24 displaced first-layer atoms, which is in good agreement with our results. This suggests that SIOA measurements probe the roughened area, i.e., individual dimers. The actual etch yield of Si(001) with 800-eV Ar ions is about[24] 0.8 Si atom/ion. Our estimate of a roughened area equivalent to 26 first-layer atoms/ion shows that most of the roughening arises from displaced Si atoms rather than from atoms removed from the surface, which is consistent with molecular-dynamics calculations.[19] The roughened area model proposed for the effect of ion bombardment turns out to be applicable in the range from a completely 2×1 dimerized surface to a fully amorphized surface layer. This shows that during etching or

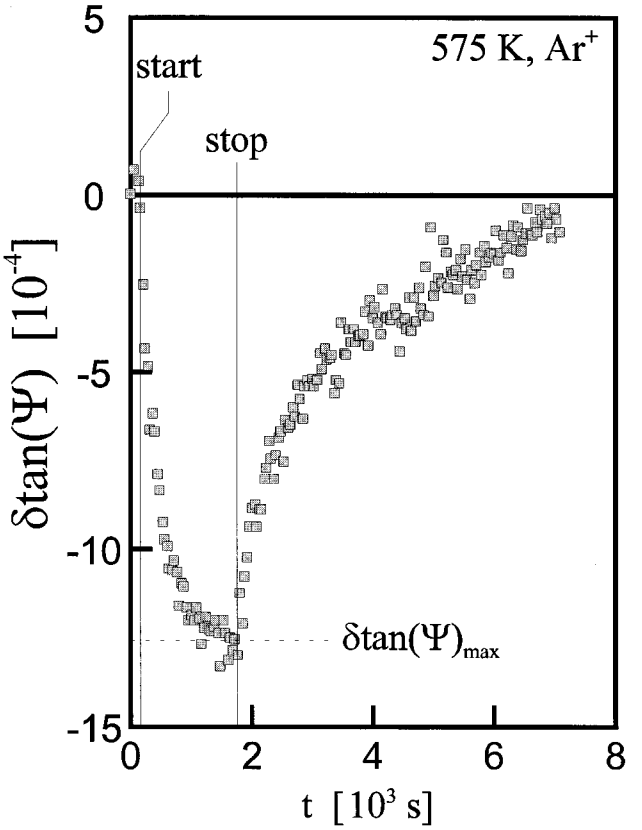

FIG. 3. δ tan(ψ) at $h\nu = 3.0$ eV before, during, and after etching at 575 ± 15 K with 800-eV Ar ions at a flux of 10^{11} ions cm^{-2} s^{-1}. See text for further details.

homoepitaxial growth the SIOA signal can be used to follow the evolution of the surface domain excess factor δf.

IV. ETCHING AT HIGHER TEMPERATURES

Single-domain surfaces were etched with the same ion flux as used in Fig. 2 in the temperature range 293–670 K. At temperatures ranging from 490 to 650 K, two effects are observed simultaneously. These effects are demonstrated in Fig. 3, where δ tan(ψ) is given during and after ion bombardment at 575 K. The first and most prominent feature is that, if ion bombardment is stopped, the SIOA signal immediately reacts by returning to its original value. This clearly shows that surface damage is annealed at these temperatures. In Fig. 3 it is clear that at 575 K all damage will anneal out in time. The recovery of the SIOA signal after ion bombardment at 575 K is consistent with the recovery of ion induced (bulk) defects at this temperature for low ion dose.[25] The recovery from ion-induced damage by annealing is intimately related to the second feature in our measurements: the maximum change in δ tan(ψ), called δ tan(ψ)$_{\max}$ hereafter, drops upon increasing the etch temperature. See Fig. 4 for the temperature dependence of δ tan(ψ)$_{\max}$. The drop in $|\delta$ tan(ψ)$_{\max}|$ has two possible origins: (i) At δ tan(ψ)$_{\max}$, distortion of the surface structure by ions and recovery of the surface structure by annealing are balanced. As a result, δf stays nearer to its original value if annealing becomes more important, e.g., if the sample temperature is higher. This agrees with our measurements which show that $|\delta$ tan(ψ)$_{\max}|$

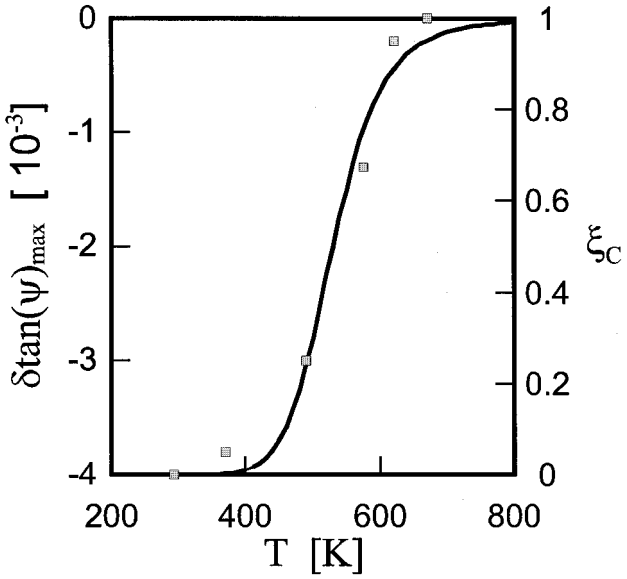

FIG. 4. Squares: δ tan(ψ)$_{\max}$ measured as indicated in Fig. 3 in the temperature range from 293 to 670 K. Etch parameters: 800-eV Ar ions at a flux of 10^{11} ions cm^{-2} s^{-1}, photon energy 3.0 eV. The full line is a fit of $\xi_C^{\rm eq}$ according to Eq. (7c).

drops rapidly between 489 and 575 K, while at 670 K there is no observable change in tan(ψ) when the sample is sputtered. (ii) The second cause for the decrease of $|\delta$ tan(ψ)$_{\max}|$ with increasing temperature may be temperature dependencies of dielectric functions. Consider a surface with an initial excess domain fraction $\delta f(0)$ and a domain excess fraction $\delta f(t)$ after sputtering for a certain time t at temperature T. The change in SIOA is given by[9,14]

$$[1+\delta\tan(\psi)]\exp(i\delta\Delta)-1 = \frac{2ieEd}{\hbar c}\,\frac{\epsilon_{[110]}(T)-\epsilon_{[1\bar{1}0]}(T)}{\epsilon_B(T)-1}[\delta f(0)-\delta f(t)]. \qquad (6)$$

The SIOA signal of Si(001)-2×1 is shown to have negligible temperature dependency in the range of[12] 293–750 K. Hence the drop in $|\delta$ tan(ψ)$_{\max}|$ with increasing temperatures

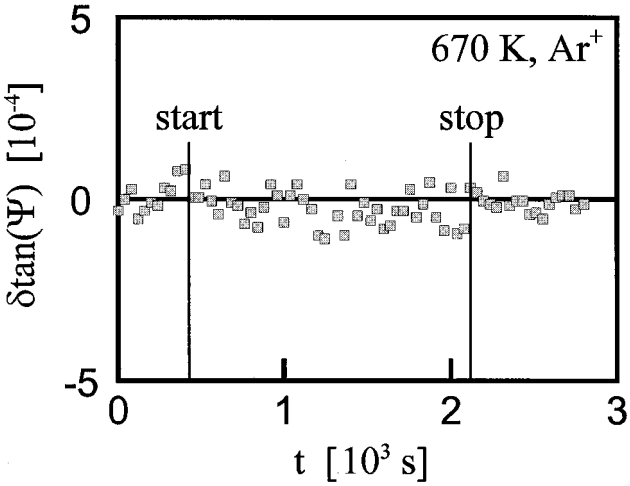

FIG. 5. δ tan(ψ) at $h\nu = 3.0$ eV during and after etching at 670 ± 15 K with 800-eV Ar ions at a flux of 10^{11} ions cm^{-2} s^{-1}.

is caused by a more single-domain surface due to annealing effects which counteract roughening by ions.

In Fig. 5, the optical anisotropy during and after Ar^+-ion bombardment at 670 K is given. It is clear that the optical anisotropy is unaffected by etching under these conditions. If, for example, D_B steps are broken and converted into a pair of S_A+S_B steps, then the domain excess fraction will decrease and the optical anisotropy changes, which is not observed. Therefore, we conclude that this surface etches by means of D_B step retraction under these conditions, and the surface stays in its equilibrium configuration. This temperature, 670 K, coincides with the temperature where bulk damage by Ar ions is reported to decrease significantly for ion fluences below[26] 5×10^{15} cm^{-2}. The value of the SIOA signal also depends on the bulk dielectric function [see Eq. (6)], and amorphization of the bulk influences the optical response. Therefore, D_B step etching can only be observed if bulk damage is absent. Also, the temperature must be sufficiently high to allow all surface defects to diffuse to the D_B step edges. At 670 K, and 10^{11} Ar ions $cm^{-2}\,s^{-1}$ at 800 eV, these conditions are fulfilled for this misorientation angle.

Since temperature effects on the SIOA signal can be neglected it is possible to calculate ξ_C from the measured values of $\delta\tan(\psi)$ in the temperature range 293–670 K. The fractions $\xi_C^{\rm eq}=\delta\tan(\psi_{\rm max})/\delta\tan(\psi_{{\rm max},T=293\ {\rm K}})$ are calculated from the left axis of Fig. 4, and yield the right axis of this figure. By doing this we implicitly assumed that the domain excess fraction of the surface before etching, $\delta f(0)$, equals unity. The data points in Fig. 4 give the fraction $\xi_C^{\rm eq}$ when roughening and annealing are in equilibrium. Taking the same model as before for roughening, i.e., the roughened area is proportional to the crystalline fraction, yields

$$\frac{d\xi_C}{dt}=-\xi_C\Phi A_S\,. \tag{7a}$$

Further, we assume annealing to be proportional to the roughened area with one single effective time constant $\tau_{\rm an}$ which is determined by an effective energy barrier $E_{\rm an}$ according to

$$\frac{d\xi_C}{dt}=\frac{1-\xi_C}{\tau_{\rm an}}=(1-\xi_C)\,\nu_{\rm an}\,\exp\left(-\frac{E_{\rm an}}{K_BT}\right), \tag{7b}$$

k_B is Boltzmann's constant and $\nu_{\rm an}$ is the attempt frequency multiplied by a proportionality factor. For the data points in Fig. 4, roughening and annealing are in equilibrium and combining Eqs. (7a) and (7b) yields

$$\xi_C^{\rm eq}=\frac{1}{1+\dfrac{\Phi A_S}{\nu_{\rm an}}\exp\left(\dfrac{E_{\rm an}}{k_BT}\right)}. \tag{7c}$$

This model is fitted to the data of Fig. 4, resulting in $\nu_{\rm an}=5.8\times10^3\ s^{-1}$, and $E_{\rm an}=0.65$ eV. As can be seen in Fig. 4, this model gives a reasonable description of $\xi_C^{\rm eq}$ with a limited number of parameters. However, ion bombardment yields various kinds of damage, like missing dimers, defect dimers, adatoms, and adclusters,[19,20] as well as bulk damage. Different types of damage will have different energy barriers and hence more time constants are involved in the anneal process. This can be seen in Fig. 3, where at least two time constants are involved. Immediately after ion bombardment has stopped, $\tau_{\rm an}\approx50$ s and at longer time scales $\tau_{\rm an}\approx2000$s. Corresponding energy barriers are 0.63 and 0.8 eV, respectively. They are of the same order of magnitude, which explains why Fig. 4 can be described with just one effective energy barrier, despite the fact that several anneal processes are involved. Furthermore, our estimates for energy barriers associated with annealing processes correspond fairly well with reported interaction energies of dimers: 0.38 eV between adjacent dimers in a dimer row and 0.24 eV between dimers in adjacent dimer rows.[27]

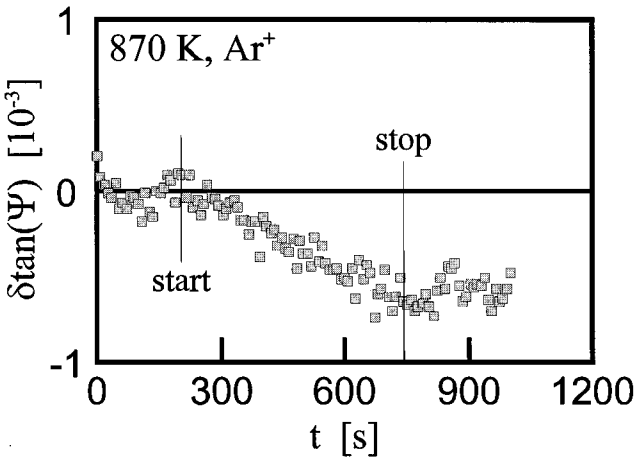

FIG. 6. $\delta\tan(\psi)$ at $h\nu=3.5$ eV upon etching with 800-eV Ar ions at sample temperature 870 ± 15 K and a flux of 7×10^{12} ions $cm^{-2}\,s^{-1}$.

In equilibrium, nominal flat Si(001)-2×1 has single steps and alternating A- and B-domain terraces. In this configuration, the stress energy is minimized while step energies only have marginal influence due to their intrinsic low densities. Then preferential incorporation at S_B steps of diffusing species during growth or etching can give a different, nonequilibrium surface morphology, like D_B steps in homoepitaxial growth[7] or D_A steps during etching.[1] On Si(001)-2×1, oriented 4.4° toward [110], the equilibrium structure is D_B stepped with B domains only. Here, the energy gain of one D_B step instead of a pair of S_A+S_B steps is large enough to compensate for the loss of strain relaxation associated with single B-domain coverage.[28] During homoepitaxial growth, preferential incorporation of Si at S_B step edges will drive the surface back to its D_B stepped equilibrium configuration. Under etching with a 800-eV Ar^+-ion flux of 10^{11} ions $cm^{-2}\,s^{-1}$ at 670 K ($\sim6\times10^{-4}$ ML s^{-1}), the surface remains in its equilibrium D_B stepped configuration. Preferential incorporation of vacancies at S_B step edges[10] would result in an energetically unfavorable single stepped surface, and under these conditions equilibrating forces counteract kinetic effects completely.

V. FACETING

If the surface is etched at higher temperatures and ion fluxes, the etch behavior changes significantly, see Fig. 6 for an experiment at 870 K and 7×10^{12} Ar ions $cm^{-2}\,s^{-1}$. During etching, the SIOA signal changes, and it remains con-

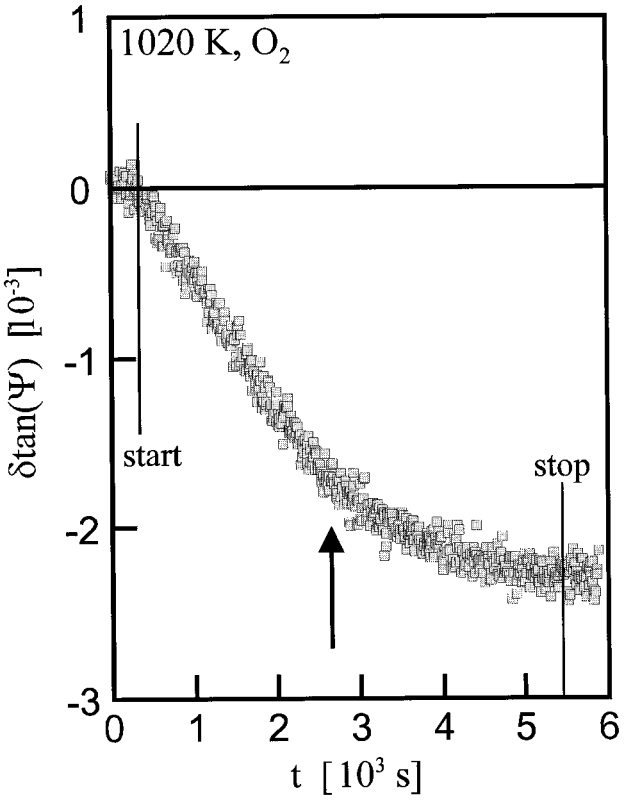

FIG. 7. $\delta \tan(\psi)$ at photon energy 3.0 eV during O_2 etching (1020 ± 15 K, 2.8×10^{-6} Pa). The arrow shows the point where the modified spectrum of Fig. 9 was recorded.

stant if sputtering is stopped, quite unlike Fig. 3, where the signal returns to its original value. This indicates that the SIOA change of Fig. 6 has to be attributed to other mechanisms than those studied in Sec. IV. Furthermore, we observed that SIOA etching experiments at 293 K, performed on substrates which were previously subjected to Ar^+ etching at 870 K, showed the same spectral behavior as in Fig. 1. However, the height of the spectrum decreases monotonously with ion fluence at 870 K. Even repeated cleaning cycles of these substrates did not yield the same height as in Fig. 1. Therefore, we conclude that during prolonged etching at 870 K the domain excess fraction δf decreases irreversibly. The same irreversible change in SIOA was observed when the surface is etched with $p_{O_2} = 2.8 \times 10^{-6}$ Pa at 1020 K; see Fig. 7. When O_2 exposure starts, the SIOA signal changes until a stable situation is reached. Stopping O_2 exposure does not affect the SIOA signal.

After the O_2 exposure of Fig. 7, we observed low-energy electron-diffraction (LEED) patterns as illustrated in Fig. 8. Around integral order spots, additional spots appear. These new spots move in the indicated directions upon variation of the electron energy. Such additional spots are consistent with spots arising from facets.[29,30] Atomic-force-microscopy (AFM) images, taken afterwards, showed several-nm-high protrusions on the surface, which is large enough to explain the additional LEED spots. Formation of pyramids has been reported during thermal etching experiments[2] at 1400 K of Si(001)-2×1. The formation of these pyramids is explained by pinning of steps at surface contaminations and the facets correspond to $\{11l\}$ planes. Presumably, pyramid formation

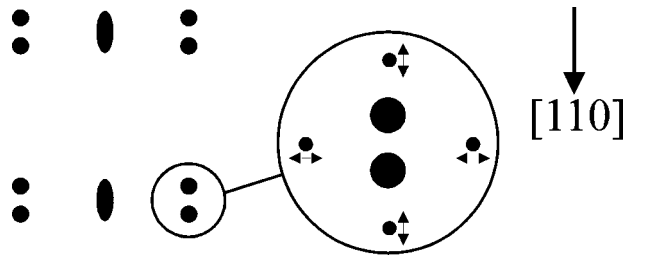

FIG. 8. Schematic LEED pattern of the surface after etching with O_2, at the arrow in Fig. 7. Spot splitting in the [110] direction is caused by regular spacing of D_B steps and half-order spots correspond to dimers on B terraces. The magnification shows additional spots moving in the indicated $\langle 110 \rangle$ directions upon variation of the electron energy.

is also the underlying cause for the change in optical anisotropy in Figs. 6 and 7, both for etching with oxygen and with Ar^+ ions.[31]

In Ref. 2, after a few second anneal treatment at 1400 K of nominal (001)-oriented Si, a random distribution of pyramids with a density of one pyramid on 9×10^4 first-layer Si atoms is found. AFM measurements, performed after the experiments of Figs. 6 and 7, show 1 protrusion on $1-2 \times 10^5$ first-layer Si atoms. The shape of these protrusions could not be resolved, but the LEED results suggest a pyramidal shape with $\{11l\}$ facets. If pyramid formation is initiated by step pinning at contaminants, and we assume a contamination level of only 0.1%, then a protrusion is initiated by a pinning center of 100 clustered foreign atoms. This contamination level is below the detection limit of standard detection techniques like AES and x-ray photoemission spectroscopy, which explains why contamination-induced pyramid formation occurs on apparently clean Si(001)-2×1. Furthermore, the etching species seems of minor importance: Besides etching with Ar ions or O_2, additional LEED spots like in Fig. 8 were also found when the sample was heated to 1020 K in a water rich environment ($p_{H_2O} = 10^{-6}$ Pa). This suggests that facet formation occurs whenever the sample is etched at elevated temperatures under conditions in which pinning centra (contaminants) are retained on the surface.

It is interesting to compare Figs. 5 and 6. The total fluence at 670 K was 25 times lower than at 870 K. The SIOA change at 870 K suggests a total change in Fig. 5 of $0.64 \times 10^{-3}/25 = 2.5 \times 10^{-4}$. The change in Fig. 5 is clearly smaller than this value. Hence a sufficiently high mobility, which allows foreign material to cluster in pinning centra, might be an essential step in the facet formation process. On nominal (001) oriented substrates, temperatures in excess of 770 K are required to reduce the number of O_2-induced step pinning centra[13] for O_2 pressures of 10^{-6} Pa. This limits the possibility of sustained D_B step etching by oxygen exposure because at 770 K the pinning centra responsible for facet formation in Fig. 6 might already be activated.

In Fig. 9 a SIOA spectrum is shown, where the initial surface is the clean, unfaceted surface and the modified spectrum is recorded at the arrow in Fig. 7. If the facets are oriented toward $\langle 110 \rangle$ directions, then pyramids are expected to be optically isotropic. This is justified by the observation that the SIOA signal, at 293 K, of a faceted surface has decreased, while no additional spectral features belonging to

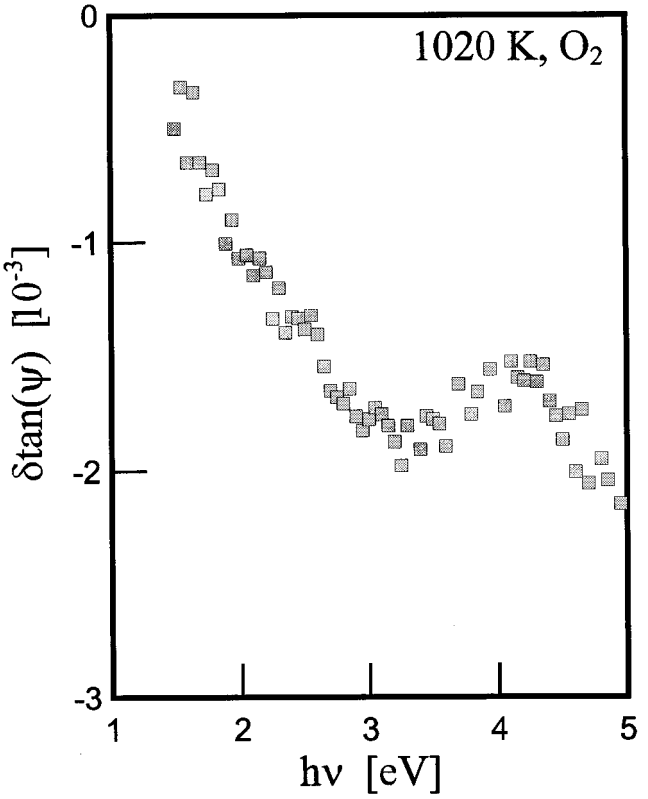

FIG. 9. Anisotropy change recorded by exposing clean single-domain Si(001)-2×1 to O_2 at sample temperature 1020 K. The modified spectrum is taken at the arrow in Fig. 7.

facets are found. Consequently, the spectrum in Fig. 9 originates from a decrease in δf on the modified surface. Thus, apart from the height, this spectrum represents optical anisotropy of dimers on Si(001)-2×1 at 1020 K. In spectra, taken at 293 and 1020 K, some common features can be identified: a large SIOA at 3.0–3.5 eV, a minimum at 4.0–4.5 eV, and an increasing SIOA at the high-energy side. Also, the spectrum at 1020 K is broadened with respect to the 293-K spectrum. Broadening of features in dielectric functions with increasing temperature is a common effect,[32] which confirms the attribution of the spectrum of Fig. 9 to surface dimers.

As discussed, facets reduce the size of the SIOA signal, but the spectral features are unaffected. It could very well be that facet formation is responsible for the different size of SIOA spectra in Refs. 9–12 and this work. The relatively large SIOA signals in this work indicate a relatively large domain excess fraction on our substrates, and the relatively low SIOA signals in Refs. 9–12 suggests that their surfaces are covered by facets and/or their surfaces are not (yet) in the equilibrium D_B stepped configuration. This emphasizes once more the importance of carefully controlling surface preparation techniques.

VI. CONCLUSIONS

Reported optical anisotropy data of Ge(001)-2×1 and Si(001)-2×1, with a misorientation angle of 4°–5° toward [110], show a large variation in size. Besides a difference in domain excess fraction, caused by small differences in misorientation angle, this variation might be due to cleaning procedures involving etching stages at high substrate temperatures. Then protrusions on the surface can be formed by pinning at residual contaminations and the remaining dimer related optical anisotropy decreases. The etching process itself seems unimportant: etching with reactive gases (O_2, H_2O), 800-eV Ar^+ ions, and even thermal etching may result in facets on the surface. Hence reliable SIOA measurements of Si(001)-2×1 are critically dependent on surface preparation techniques, and an etching stage at elevated temperatures should be avoided. SIOA measurements at 1020 K, where the dimerized area is reduced by facet formation, and at 293 K, where the surface is roughened by incident ions, display similar spectral features. This indicates that the measured anisotropy changes at 1020 K are related to a reduction of the domain excess fraction δf.

At 293 K, the evolution of the SIOA signal during 800-eV Ar^+ etching can be described with a simple model where one ion roughens an area corresponding to 26 ± 2 first-layer Si atoms. Comparing the actual etch rate of ~ 0.8 Si atom/ion to the roughened area of 26 first-layer Si atoms/ion reveals that, at 293 K, the SIOA signal is dominated by roughening rather than Si removal. Increasing the substrate temperature during etching with 10^{11} Ar^+ ions $cm^{-2}s^{-1}$ reveals that annealing processes reduce the change in optical anisotropy. This maximum SIOA change under etching conditions could be described by a straightforward model with two effective parameters. The anneal behavior at 575 K reveals a number of time constants and consequently various anneal processes play a role. At 670 K and 10^{11} Ar^+ ions $cm^{-2}s^{-1}$, the surface remains in its equilibrium structure, i.e., the surface etches in the D_B step retraction mode. Facet formation during etching at higher temperatures inhibits the range of conditions where D_B step retraction will occur.

ACKNOWLEDGMENTS

This work is part of the research of the Stichting voor Fundamenteel Onderzoek der Materie (FOM), which is financially supported by the Nederlandse Organisatie voor Wetenschappelijk Onderzoek (NWO). One of the authors, H.W., acknowledges the Royal Netherlands Academy of Science (KNAW) for their support.

[1] P. Bedrossian and T. Klitsner, Phys. Rev. Lett. **68**, 646 (1992).

[2] Ch. Ziegler, A. W. Munz, and W. Göpel, Surf. Sci. **325**, 177 (1995).

[3] J. Greene, S. Barnett, J. Sundgren, and A. Rockett, in *Ion Beam Assisted Film Growth*, edited by T. Itoh (Elsevier, Amsterdam, 1989), p. 101.

[4] D. E. Aspnes, Appl. Phys. Lett. **62**, 1343 (1993); J. Opt. Soc. Am. A **10**, 974 (1993).

[5] S. R. Armstrong, R. D. Hoave, M. E. Pemble, I. M. Povey, A. Stafford, A. G. Taylor, B. A. Joyce, J. H. Neave, D. R. Klug, and J. Zhang, Surf. Sci. **274**, 263 (1992).
[6] F. K. Men, W. E. Packard, and M. B. Webb, Phys. Rev. Lett. **61**, 2469 (1988).
[7] A. J. Hoeven, J. M. Lenssinck, D. Dijkkamp, E. J. van Loenen, and J. Dieleman, Phys. Rev. Lett. **63**, 1830 (1989).
[8] E. Pehlke and J. Tersoff, Phys. Rev. Lett. **67**, 1290 (1991); J. J. de Miguel, C. E. Aumann, R. Kariotis, and M. G. Lagally, *ibid.* **67**, 2830 (1991).
[9] T. Yasuda, L. Mantese, U. Rossow, and D. E. Aspnes, Phys. Rev. Lett. **74**, 3431 (1995).
[10] L. Kipp, D. K. Biegelsen, J. E. Northrup, L.-E. Swartz, and R. D. Bringans, Phys. Rev. Lett. **76**, 2810 (1996).
[11] U. Rossow, L. Mantese, and D. E. Aspnes, J. Vac. Sci. Technol. B **14**, 3070 (1996).
[12] R. J. Cole, S. Tanaka, P. Gerber, J. R. Power, T. Farrell, and P. Weightman, Phys. Rev. B **54**, 13 444 (1996).
[13] C. Pearson, B. Borovsky, M. Krueger, R. Curtis, and E. Ganz, Phys. Rev. Lett. **74**, 2710 (1995).
[14] D. J. Wentink, Ph.D. thesis, University of Twente, Enschede, The Netherlands, 1996.
[15] D. J. Wentink, M. Kuijper, H. Wormeester, and A. van Silfhout, Rev. Sci. Instrum. **67**, 1947 (1996).
[16] D. J. Wentink, H. Wormeester, P. L. de Boeij, C. M. J. Wijers, and A. van Silfhout, Surf. Sci. **274**, 270 (1992).
[17] H. Wormeester, D. J. Wentink, P. L. de Boeij, C. M. J. Wijers, and A. van Silfhout, Phys. Rev. B **47**, 12 663 (1993).
[18] The shape of optical anisotropy spectra in Refs. 17 and 9 is identical, while the size in Ref. 17 is substantially larger. This can be attributed to a difference in domain anisotropy caused by a slightly different misorientation angle. The sign of $\delta \tan(\psi)$ in Ref. 17 is indeed incorrect, as pointed out in Ref. 9. After correcting this, the signs of the spectra match.
[19] H. Feil, H. J. W. Zandvliet, M. H. Tsai, J. D. Dow, and I. S. T. Tsong, Phys. Rev. Lett. **69**, 3076 (1992).
[20] H. J. W. Zandvliet, H. B. Elswijk, E. J. van Loenen, and I. S. T. Tsong, Phys. Rev. B **46**, 7581 (1992).
[21] H. Wormeester, D. J. Wentink, and A. van Silfhout, Phys. Rev. B **56**, 3617 (1997).
[22] C. M. J. Wijers and G. P. M. Poppe, Phys. Rev. B **46**, 7605 (1992).
[23] D. E. Aspnes, Y. C. Chang, A. A. Studna, L. T. Florez, H. H. Farrell, and J. P. Harbison, Phys. Rev. Lett. **64**, 192 (1990).
[24] P. C. Zalm, J. Appl. Phys. **54**, 2660 (1983).
[25] A. H. Al-Bhayati, K. G. Orrman-Rositter, R. Badheka, and D. G. Armour, Surf. Sci. **237**, 213 (1990).
[26] L. J. Huang, W. M. Lau, H. T. Tang, W. N. Lennard, I. V. Mitchell, P. J. Schultz, and M. Kasrai, Phys. Rev. B **50**, 18 453 (1994).
[27] H. J. W. Zandvliet, H. B. Elswijk, E. J. van Loenen, and D. Dijkkamp, Phys. Rev. B **45**, 5965 (1992).
[28] H. J. W. Zandvliet, S. van Dijken, and B. Poelsema, Phys. Rev. B **53**, 15 429 (1996).
[29] G. Ertl and J. Küppers, *Low Energy Electrons and Surface Chemistry* (Verlag Chemie, Weinheim, 1974).
[30] The same additional LEED spots are found when the sample is heated to 1020 K in a water rich environment $p_{H_2O} < 10^{-6}$ Pa.
[31] H. F. Dylla, J. C. King, and M. J. Cardillo, Surf. Sci. **74**, 141 (1978).
[32] G. Vuye, S. Fisson, V. Nguyen Van, Y. Wang, J. Rivory, and F. Abelès, Thin Solid Films **233**, 166 (1993).